Fluorescence spectrum of Mo2 in argon and krypton matrices

M. J. Pellin, T. Foosnaes, and D. M. Gruen

Citation: The Journal of Chemical Physics **74**, 5547 (1981); doi: 10.1063/1.440917
View online: http://dx.doi.org/10.1063/1.440917
View Table of Contents: http://scitation.aip.org/content/aip/journal/jcp/74/10?ver=pdfcov
Published by the AIP Publishing

Fluorescence spectrum of Mo_2 in argon and krypton matrices[a)]

M. J. Pellin, T. Foosnaes, and D. M. Gruen

Chemistry Division, Argonne National Laboratory, Argonne, Illinois 60439
(Received 24 December 1980; accepted 30 January 1981)

The time resolved fluorescence spectra of Mo_2 isolated in Ar and Kr matrices at 14 °K are presented. Depending on excitation wavelength, either of two separate vibrational progressions with 475.7 (±4.5) cm^{-1} spacings can be observed in emission. Similarities between several features in the two emission spectra lead to the conclusion that the progressions arise from Mo_2 trapped in two distinct sites, each characterized by its own absorption spectrum. Excitation spectra elucidate the overlapping absorption spectra of the two sites. The measured emission lifetimes are long and not single exponential. In krypton matrices, lifetimes of 0.85 msec from one site and a biexponential emission decay of 0.70 and 1.94 msec from a second site are observed. In argon matrices, 2.1 msec emission decay times in one site and a triexponential decay with components of 2.1, 3.93, and 6.3 msec were measured in a second site. Phonon structure in the well resolved spectra show that the matrix coupling is different for the two matrix sites. Various empirical correlation rules are used to test the validity of ω_e as well as to compare it to other experimental quantities for Mo_2. These rules indicate a 1.9 Å bond length for Mo_2. The fluorescence lifetimes and the large spectral shift of the emission relative to the excitation energy lead to the conclusion that the emission does not emanate from the initially excited level. Instead, the emission appears to come from one of the higher spin multiplicity levels in a dense manifold of states lying at somewhat lower energies than the $^1\Sigma_u^+$ level coupled by laser radiation to the $^1\Sigma_g^+$ ground state.

I. INTRODUCTION

Transition metal clusters ranging from a few to a few hundred atoms play a key role in such diverse areas as nucleation phenomena,[1] photography,[2] and catalysis.[3] For catalysis these clusters not only represent a new class of specific, active catalytic species[4] in organometallic compounds, but they also are models for adsorbate–adsorbent interactions in heterogeneous catalysis.[5,6] In each of these areas of interest, and catalysis in particular, the properties of the metal–metal bond play a key role. The *d*-electron character of transition metal bonding provides a variety of unusual characteristics including high spin multiplicities, dense manifolds of low lying states, high bond orders and high dissociation energies.[7] In transition metal organo-metallics containing multiple metal–metal bonds, a variety of ligand substitution and addition reactions have been demonstrated.[8] Indeed, it has been suggested that substitution reactions at the metal–metal multiple bond are an integral part of the specific catalytic activity of several unsaturated transition metal cluster compounds.[8]

Diatomic molybdenum is particularly interesting in this regard. Organo-metallics containing molybdenum–molybdenum bonds have bond orders ranging from 3 in $Mo_2Cl_8^{4-}$[9] and $Cp_2Mo_2(CO)_4$[8] to 4 in $Mo_2(O_2CCH_3)_4$[10] and $Mo_2(PhNC(O)CH_3)_4$.[11] Calculations suggest that the naked metal cluster has a bond order as high as 6.[7,12–17] Correspondingly, the equilibrium molybdenum–molybdenum bond distance r_e is found to vary from an exceptionally short 2.1 Å in $Mo_2Cl_8^{4-}$[9] to 3.39 Å in $Cp_2Mo_2(CO_4)_4$.[8] Many of these compounds are found to display catalytic activity. In the present study the metal diatomic Mo_2 isolated in rare gas matrix supports will be investigated using time resolved laser fluorescence spectroscopy.

Mo_2 was first detected as a new absorption feature at ~520 nm which appeared upon thermal annealing of molybdenum-doped argon and krypton matrices.[18] Further characterization of this molecule carried out by several groups[13,19–22] identified two weaker absorption bands at 308 and 232 nm.[20,21] The main absorption feature at 520 nm shows structure that varies with annealing.[17,21] This structure is perplexing since the features within it have neither regular spacings nor similar shapes. In argon and krypton matrices, under some conditions of matrix preparation, an average spacing of 181 cm^{-1} for this 520 nm absorption has been observed[22] which can be compared to that reported for CrMo of 147 cm^{-1}.[13]

Gas phase spectroscopic measurements have been reported for Mo_2 molecules produced by flash photolysis of $Mo(CO)_6$.[23–27] The absorption spectrum 50 μsec after photolysis shows a band at 519 nm which has been assigned to Mo_2.[23–27] The feature is perplexing in that it shows a regular absorption peak progression with an ~18 cm^{-1} spacing. Emission from the photolyzed carbonyl has been analyzed by two groups. One group[24] interpreted the $A\,^1\Sigma^+$ emission band observed at 519 nm as corresponding to a 40 cm^{-1} vibrational energy spacing. In a more extensive analysis of the emission spectrum,[23] two new bands designated *B* and *C* at ~390 and 314 nm respectively were observed as well as the $A\,^1\Sigma^+$ emission at 519 nm. The *A* band emission shows a group of peaks with a 33 cm^{-1} spacing, assigned as a $\Delta v = 0$ sequence. Thus the spacing most likely represents the difference between ground and excited state ω_e's. This assignment is based on progressions in the *B* and *C* emissions which show spacings of 477.1 cm^{-1}. Unfortunately, none of the vibrational progressions are well resolved and no ground state vibrational level higher than $v'' = 4$ is observed. It should be noted that

[a)]Work performed under the auspices of the Office of Basic Energy Sciences, Division of Materials Sciences, U. S. Department of Energy.

 0021-9606/81/105547-11$01.00

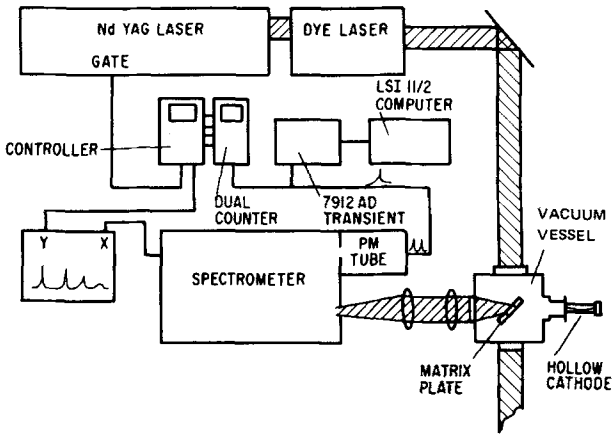

FIG. 1. Apparatus used to measure laser induced fluorescence spectra.

the 477.1 cm^{-1} value for the ground state vibrational spacing of gas phase Mo_2 is not in agreement with preliminary Raman measurements of matrix isolated Mo_2[20] which indicate $\omega_e = 315$ cm^{-1}.

Calculations using extended Hückel[12] and SCF–Xα–SW[7,13,16] techniques have identified the ~520 nm absorption feature as a $^1\Sigma_g^+ - {}^1\Sigma_u^+$ transition. *Ab initio* theoretical calculations of the Mo_2 electronic structure are difficult due to the high multiplicities possible in a bonding scheme involving two $d^5 s^1$ atoms. Recently several *ab initio* calculations on the $^1\Sigma_g^+$ ground state of Mo_2 have been reported.[14,15,17] These calculations indicate bond lengths of 2.02 Å[15] and 1.97 Å[14] and ground state vibrational frequencies of 388 cm^{-1}[14] and 475 cm^{-1},[15] respectively. It is important to note that the calculations[14,15] give much lower binding energies than measured for Mo_2 by mass spectrometric methods.[28] Multiconfiguration self-consistent field methods with configuration interaction are evidently accurate only near the equilibrium internuclear distance. In one calculation no attempt was made to determine the well depth,[14] while it was predicted to be 20 kcal mol^{-1} in the other calculation,[15] in serious disagreement with the experimental value of 95 kcal mol^{-1}.[28] Extensive *ab initio* calculations presently being made include the excited state structure of Mo_2 and indicate that the first optically allowed state above the $^1\Sigma_g^+$ ground state is a $^1\Sigma_u^+$ state.[29] Analogy between the excited state structure of Mo_2 and that of Cr_2, on which extensive calculations have been performed,[30] can be drawn as well. In particular it is interesting to note that the free atom states which give rise to the $^1\Sigma_g^+$ ground state of Mo_2 also can form into a manifold of higher multiplicity states (e.g., $^3\Pi_u^+$, $^5\Sigma_g^+$, ...) which must lie above it. Similarly by analogy with Cr_2[30] the $^1\Sigma_u^+$ excited state of Mo_2 must lie to higher energies than the manifold of higher multiplicity states which form from the geminate free atom states.

The purpose of the present series of investigations was to determine the molecular parameters of Mo_2 in ground and excited states. This information will be useful as a probe of the Mo–Mo bond. A future goal is to examine reactions of Mo and Mo_2 with small molecules in matrices so as to be able to study changes in the Mo–Mo bond in situations of potential interest to catalysis.

II. EXPERIMENTAL

The laser fluorescence apparatus consisted of a laser excitation source, a detection system, and a matrix apparatus which included a metal generation source (Fig. 1). A Molectron MY34-DL16 unstable Nd:Yag laser-dye laser system was used as an excitation source. The system produces 15 nsec dye laser pulses which are not temporally smoothly varying, but rather show the two-peak, mode beating behavior characteristic of unstable Nd:Yag laser systems. The laser frequency width was generally about 0.75 Å. However, no change in the emission spectra could be detected upon etalon insertion which narrowed the bandwidth to 0.008 Å. The energy of the excitation pulse (with C500 laser dye) in the 490–540 nm range could be increased to 10 mJ/pulse. In general, energies of 0.1 mJ were sufficient to saturate fluorescent emission.

The laser pulse was directed onto the front surface of the matrix plate at right angles to the detection equipment (see Fig. 1). Emission from the matrix was collected and then focused on the slits of a 1 m Czerny–Turner spectrometer. The ultimate resolution of the spectrometer was ≤ 0.3 Å. Light at the exit slit of the spectrometer was detected with a C31034A RCA photomultiplier tube in a cooled housing. The output of the photomultiplier could be monitored either by a Tektronics 912AD transient digitizer interfaced to an LSI 11/2 microcomputer or by a gated photon counting system. The transient digitizer could monitor lifetimes as short as the laser pulse itself. For the long lifetimes of the transitions measured here, it was found that the photon counting unit used in a boxcar mode produced more accurate results. The low quantum yields also made photon counting desirable.

The matrix apparatus consisted of a 25 mm diameter, 2 mm thick sapphire deposition plate secured to a copper block with indium seals. Temperatures at the bottom of the block were monitored with a cryogenic diode sensor. The minimum temperature of 14 °K was maintained throughout deposition and spectroscopic analysis by a Cryodyne Cryocooler (Model 21) closed cycle helium refrigerator. The matrix plate was located in a vacuum dewar with 10^{-7} Torr base pressure. The dewar had three windows allowing both absorption and fluorescence experiments to be conducted. Research grade Ar and Kr gases were used as received. Gas deposition rates were maintained at a constant rate in the range 8–15 mmol/h by a calibrated flow meter.

The source of metal atoms was a sputtering device consisting of a Mo hollow cathode and a Pt anode.[31] A chief advantage of this source is that it generates Mo atoms without heating the metal to a high temperature. Estimated Mo/M ratios, where M is the matrix gas, varied in the range 10^{-4}–10^{-3}. Deposition times varied from 5 to 30 min.

Cluster species of molybdenum could only be generated under carefully controlled conditions. Not only the

Mo/M ratio, but also the deposition rate had to be monitored. This indicates that cluster formation occurs chiefly on the growing matrix surface before thermal accomodation is complete. Only slight changes in deposition conditions produced absorption spectra denoting the presence either only of atoms or of various combinations of atoms, diatomics, higher clusters, and colloidal metal.

In order to insure the invariance of matrix samples during fluorescence experiments, as well as to characterize the matrix itself, absorption spectra were taken before and after each experiment. Changes in absorption spectra upon thermal annealing have been demonstrated previously.[22] However, changes in either the fluorescence or absorption spectra were found to be minor when the Mo_2 peak was photo-annealed. After the first few minutes of irradiation, the absorption and emission peak shapes remained invariant even after many hours of irradiation. The changes that occur in the initial photo-annealing experiments in Ar can be characterized as due to a small loss in intensity of the 533 nm peak in absorption and a change in the Franck–Condon factors for emission making the second emission peak more intense than the highest energy emission peak. All spectra displayed here were recorded after the initial photo annealing period.

The stability of the absorption band of Mo_2 upon photoexcitation is in contrast to that exhibited by any of several atomic lines which are rapidly photo-bleached. In low Mo/M matrices, a concomitant growth in the Mo_2 absorption band is observed. At slightly higher Mo/M ratios, growth of another lower energy band is detected after irradiating the monomer absorptions. This band had previously been identified as Mo_3.[21]

III. RESULTS

The absorption spectrum of an Mo-doped Ar matrix is shown in Fig. 2. The most intense features have been associated with Mo atoms.[18] In particular the well-resolved triplet at ~350 nm and the less well-resolved

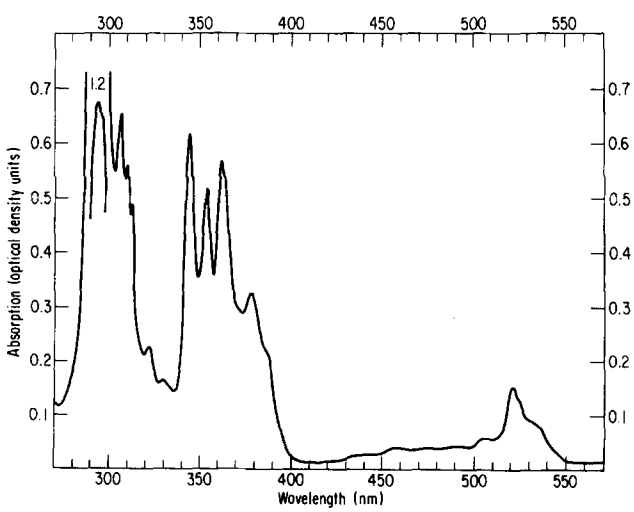

FIG. 2. Absorption spectrum of Mo doped Ar matrix. The feature of ~518 nm has been identified as Mo_2.

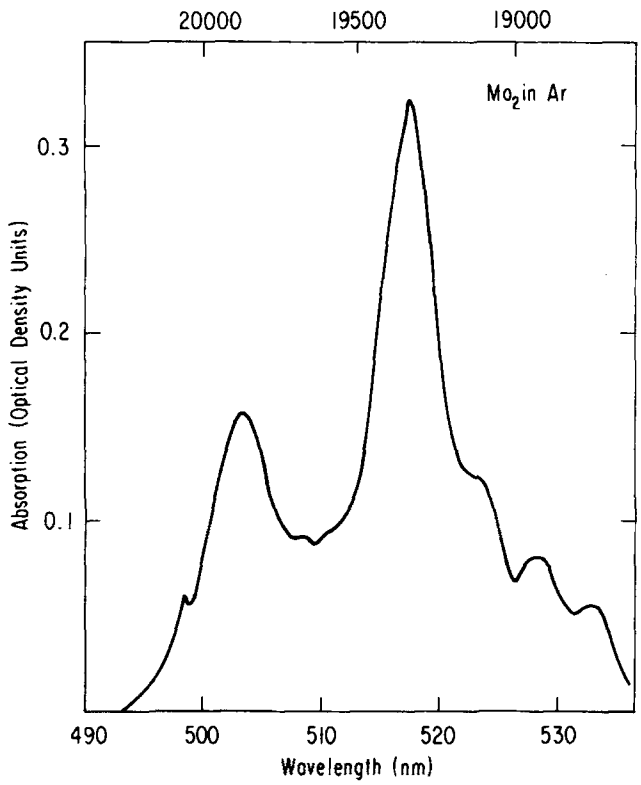

FIG. 3. Absorption spectrum of Mo_2 molecules in Ar matrix at 13°K.

triplet at 290 nm are assigned to the $z\,^7P \leftarrow a\,^7S$ and the $y\,^7P \leftarrow a\,^7S$ atomic transitions. The magnitude of the splittings in these peaks have been interpreted as due to the effect of the matrix environment on the spin–orbit coupling and configuration interaction of Mo atoms.[18] Smaller absorption peaks on the low energy side of these triplets have recently been identified as due to Mo atoms in a second matrix site.[32]

A carefully determined absorption spectrum of the feature in the 490–540 nm region, previously identified as Mo_2,[18–22] is shown in Fig. 3. In agreement with earlier experiments, we find that upon thermal annealing the atomic absorptions bleach more rapidly than the dimer feature. Furthermore, photo-diffusion experiments involving excitation of Mo atoms at 355 nm show a rapid decrease in the Mo absorption intensity while the 518 nm dimer absorption exhibits an increasing intensity during the irradiation, thus lending additional support to the assignment of this feature as Mo_2. Examination of Fig. 3 shows that the band structure lacks regular spacings and the peaks have widely varying shapes.

While excitation at 517.8 nm produces no detectable emission in the 518–690 nm spectral region, highly structured emission is observed in the 690–880 nm wavelength region as illustrated in Fig. 4. The twin peaks at 690.5 and 692.2 nm represent long lived emission resulting from excitation of the sapphire matrix plate itself. The emission, probably from Cr^{3+}, is useful as a fiducial wavelength marker as well as for apparatus alignment.

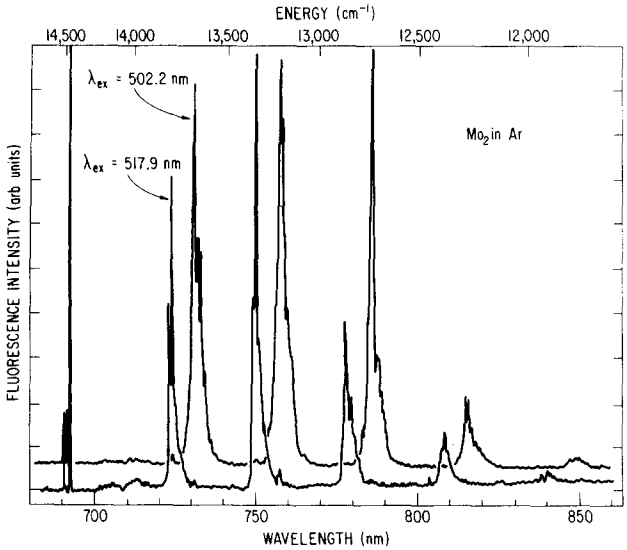

FIG. 4. Emission spectrum of Mo_2 in an Ar matrix. The upper curve is observed for 517.8 nm excitation. The lower curve results from 502.2 nm excitation.

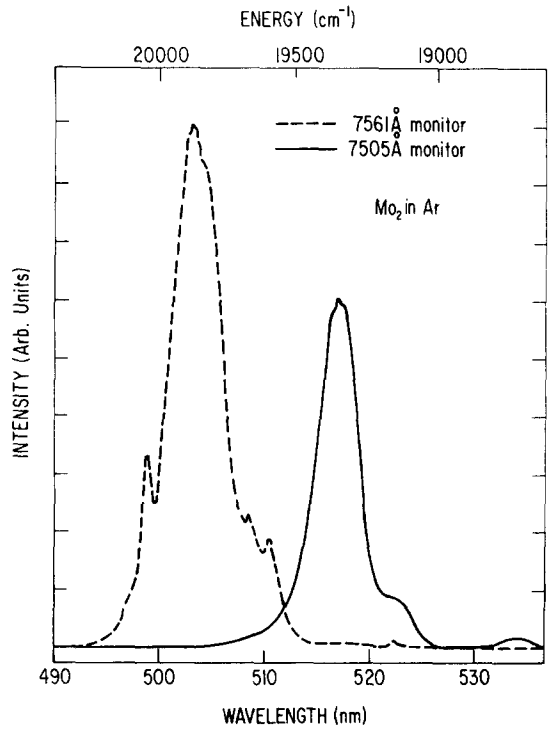

FIG. 5. Excitation spectra of Mo_2 in Ar. Solid curve is obtained by monitoring emission at 750.5 nm and scanning the excitation frequency. The broken line is derived similarly except emission was monitored at 757.1 nm.

The fluorescence spectrum in the 720–860 nm spectral region can be assigned to the Mo_2 molecule. Excitation at 522.9, 533.6, 540.5, or 543.3 nm produce an identical emission spectrum which will be labeled "red" site emission. Excitation at 502.2, 507.8, and 498.2 nm gives a different emission spectrum that will be referred to as "blue" site emission. Excitation at 507.8 nm produces a small component identical to red site emission. Both spectra displayed in Fig. 4 show progressions which are quite regular. The exact peak positions and spacings are presented in Table I. While shifted with respect to one another, the two emission spectra are remarkably similar even with regard to the Frank–Condon factors which differ only slightly.

Careful comparisons between the two emission spectra can be made in several ways. Perhaps the most striking comparison is displayed in Fig. 5 where excitation or "action" spectra are developed by scanning the excitation wavelength through the absorption band while monitoring emission at a single wavelength. There can be little doubt that the "red" and "blue" emission spectra are due to different matrix sites occupied by Mo_2 and that the complicated Mo_2 absorption spectrum represents the superposition of the spectra of the dimer in the two sites. In general, the intensities of the fluorescence spectra should mirror the absorption spectrum of the species responsible for the emission being monitored. Since excitation spectra do not monitor the absorption spectrum directly, several processes which can alter the comparison need to be considered. For example, if absorption features have different quantum yields for emission, then the relative absorption intensities will not be accurately reflected in the excitation spectrum.

TABLE I. Emission data of Mo_2 in an Ar matrix at 13.5°K.

Emission λ(Å)	Emission ν(cm⁻¹)	Excitation λ(Å)	Transition[c] ν′→ν″	FWHM (cm⁻¹)	$\Delta\nu = \nu_1'' - \nu_{1+1}''$ (cm⁻¹)	
7244.6	13803.4	5140	0→0	3.1		
7505.0	13324.5	5140	0→1	9.6	478.9	
7781.3	12851.3	5140	0→2	17.9	473.2	
8079.2	12377.5	5140	0→3	28.4[a]	473.8	$\Delta\nu = 473.2 \pm 5$ cm⁻¹
8395.9	11910.6	5140	0→4	...*	466.9	
7308.1	13682.5	5022	0→0	2.9		
7571.2	13207.9	5022	0→1	8.3	474.6	
7858.5	12725.1	5022	0→2	17.4	482.8	
8160.8	12253.7	5022	0→3	30.5[a]	471.4	$\Delta\nu = 477.9 \pm 6$ cm⁻¹
8495.6	11770.8	5022	0→4	...[b]	482.9	

[a]The zero phonon line is not well resolved.
[b]The zero phonon line is not resolved.
[c]Tentative assignment.

The excitation spectrum in Fig. 5 was produced with saturating excitation pulses which changed no more than 10% in intensity over this spectral range. It can be seen that the relative intensities for emission from the two sites are different. Indeed a rough measure of the relative quantum yields can be found by adjusting the relative emission peak heights to the corresponding absorption intensity at that wavelength. Clearly the blue site emission has about four times larger quantum yield than the red site. The absolute magnitude of the quantum yield was found to vary from matrix to matrix. Comparison with emission intensities from a quantum standard (cresyl violet)[33] fixed the yield (photons absorbed/photons emitted) in the 10^{-5} range. The absence of the 528.9 nm absorption peak in the excitation spectrum should also be noted.

A second major distinguishing feature in addition to differences in quantum yield between the emission spectra from the two sites are the fluorescent lifetimes. Figure 6 displays the emission decay rates. Excitation at 502.2 nm (blue site) results in an emission lifetime of 2.1 ± 0.2 msec regardless of the blue site fluorescence peak which is being monitored. Similar emission lifetimes are observed by excitation at 498.2 or 507.8 nm. By contrast, excitation at 517.8 nm (red site) gives a decay curve which can be analyzed in terms of the separate processes with lifetimes of 2.1, 3.4, and 6.3 msec, respectively. The decay curve is the same at this level of resolution for emission monitored at 727.4, 753.5, 781.2, or 811.5 nm. Further careful measurements at various wavelengths within the 753.5 nm peak produce no significant lifetime differences.

A final comparison between the two Mo_2 emission systems can be drawn from high resolution spectra of the emission peak shapes. Figure 7 presents a comparison of the highest energy fluorescence peaks produced by excitation into either the red or blue absorption sites. We interpret the structure as due to a strong zero phonon line followed by phonon band structure. The structure is more intense for red site emission, indicative of a larger shift along the phonon axis between the emission level coupled to the red site absorption.[29] The zero phonon lines full-widths at half-maximum (see Table I) of 3.1 and 2.9 cm^{-1} should be compared to the absorption peaks which have FWHM's ~200 cm^{-1}.

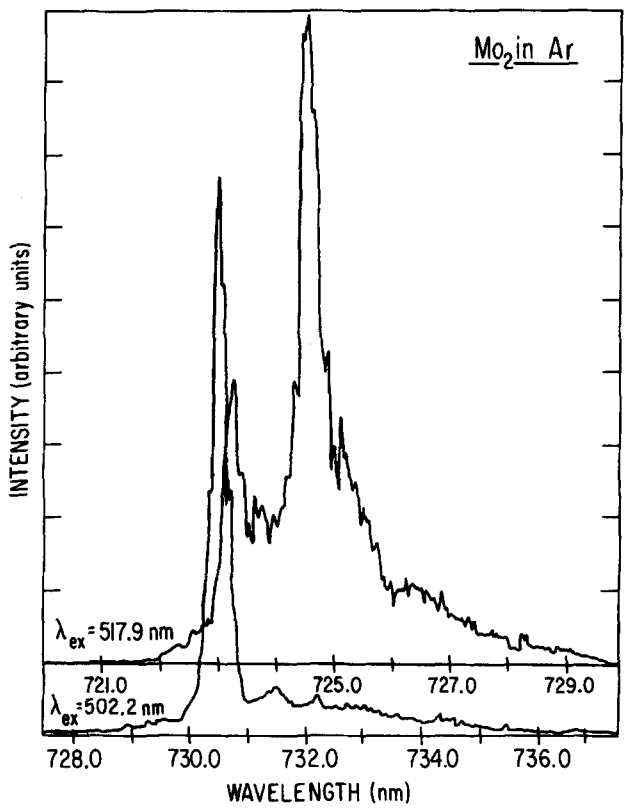

FIG. 7. Comparison of emission peak shapes produced from Mo_2 in an Ar matrix with 517.8 and 502.2 nm excitation. The peaks are the highest energy of the respective progressions.

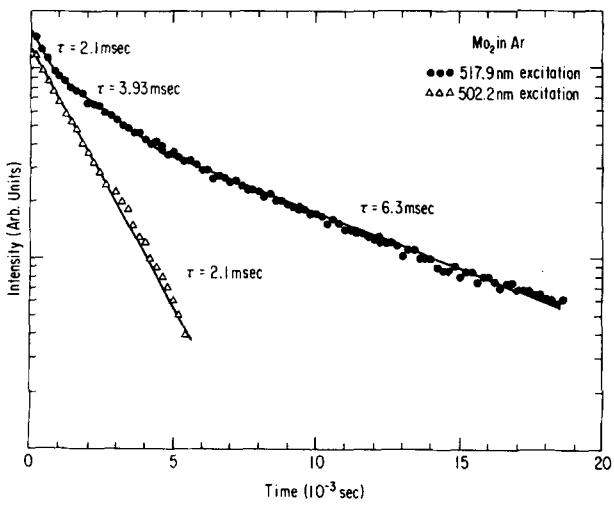

FIG. 6. Lifetime of emission at 757.1 nm produced by excitation at 517.8 nm is shown with the solid curve (○). 750.5 nm emission decay is displayed with the broken line (Δ). Excitation wavelength was 502.2 nm.

Figure 8 illustrates that the same situation obtains for the next highest energy emission peaks found at 750.5 and 757.1 nm except that the zero phonon lines have broadened making it more difficult to separate them from their respective phonon side bands. The broadening increases for emission peaks occurring at progressively lower energies. As a result the exact zero phonon line energy as well as FWHM becomes progressively more difficult to determine. Nonetheless, in every instance the emission peaks are much sharper than their corresponding absorption peaks.

The absorption spectrum of an Mo-doped Kr matrix is shown in Fig. 9. As in Ar, the most intense features have been identified with Mo atoms.[18] The features at ~350 and 290 nm represent the matrix split $Z\,^5P \leftarrow a\,^7S$ and $y\,^7P \leftarrow a\,^7S$ atomic transitions. In Kr it is apparent, as has been pointed out in earlier work, that the "red" Mo atom absorption site is present in lower abundance than in Ar.[32] The Mo_2 absorption feature[18–22] in Kr shows quite different structure than in Ar (Fig. 10) with the peaks due to "blue site" stronger and sharper relative to "red" site absorption. Again, as in Ar, photo bleaching with a 355 nm pulse produces increases in Mo_2 absorption intensities for matrices with low Mo/Kr

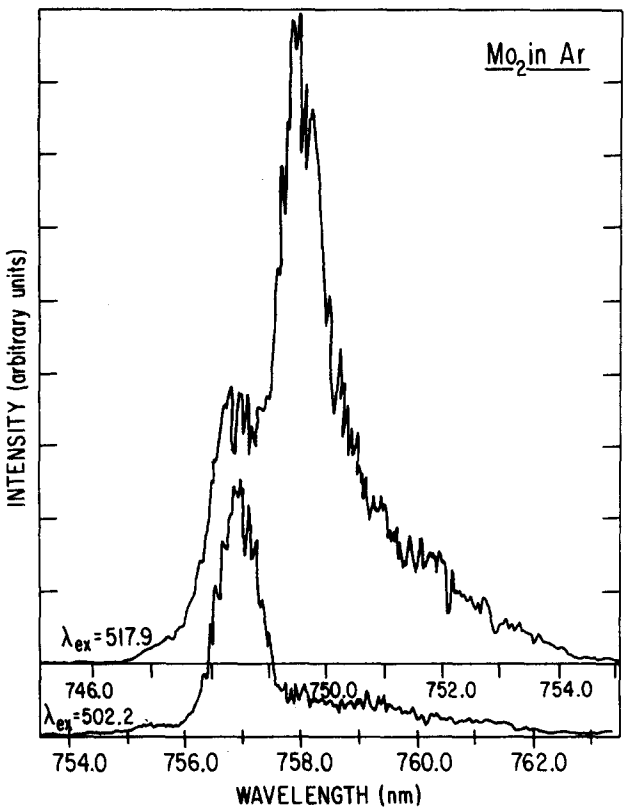

FIG. 8. Comparison of emission peak shapes of Mo_2 in an Ar matrix with 502.2 and 517.8 nm excitation. The peaks are the second highest energy emissions of the respective progressions.

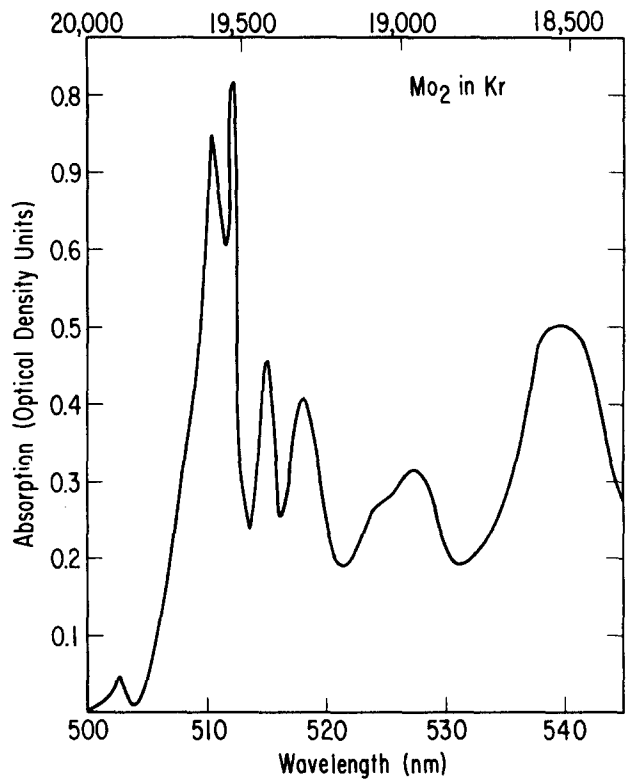

FIG. 10. Absorption spectrum produced by Mo_2 in a Kr matrix at 13°K.

ratios. If these photo bleaching experiments are run at 30°K then the difference spectrum (absorbance after irradiation-absorbance before irradiation) displayed in Fig. 11 is produced. The spectrum indicates the presence of two Mo_2 species as in Ar. It also shows that the red site is thermally more stable than the blue site.

The presence of two distinct Mo_2 species in Kr matrices is further demonstrated by laser induced emission experiments. Figure 12 is representive of the emission produced by excitation throughout the Mo_2 absorption region except for excitation at 540 nm. As with Ar matrices, either of two distinct sets of emissions are observed from Mo_2 in a Kr matrix. Excitation at 504.2, 510.9, 511.9, and 514.9 nm produces a regular progression of emission peaks whose exact position can be found in Table II. Excitation at 524.7 or 537.4 nm produces a similar but spectrally shifted emission progression (see Table II for peak positions). It is clear from Fig. 12 that the Franck–Condon factors for emission are different for the two progressions seen in emission.

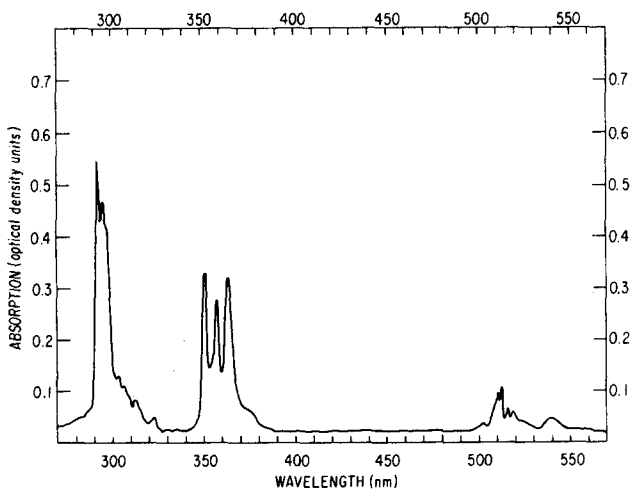

FIG. 9. Absorption spectrum of a Mo doped Kr matrix. The feature in the 490–540 nm region has been assigned to Mo_2.

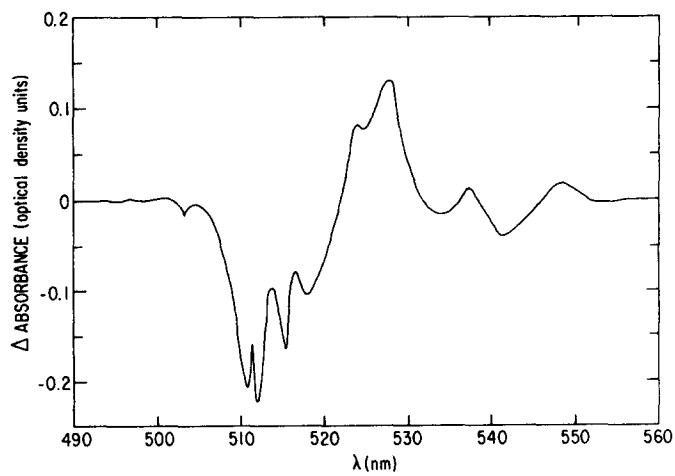

FIG. 11. Difference spectrum of Mo_2 absorption produced by subtracting the absorption spectrum of the matrix after irradiation from that taken before irradiation. Irradiation was at 355 nm for 30 min while the matrix was at 30°K.

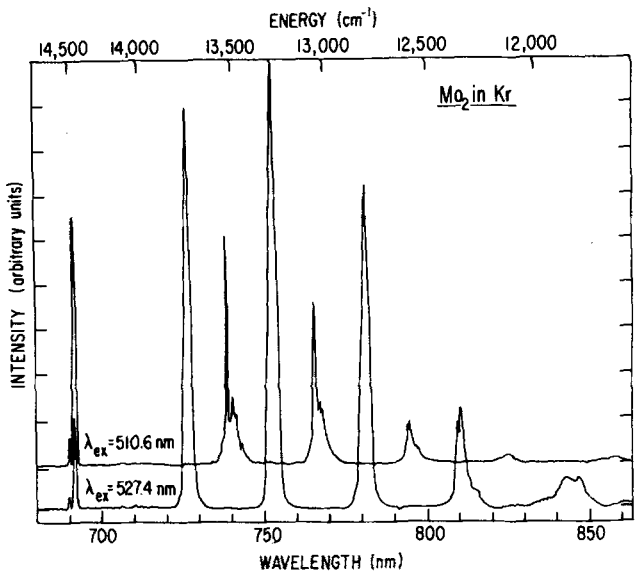

FIG. 12. Emission spectrum of Mo_2 in a Kr matrix. The upper curve is observed for 510.6 nm excitation and the lower for 527.1 nm excitation.

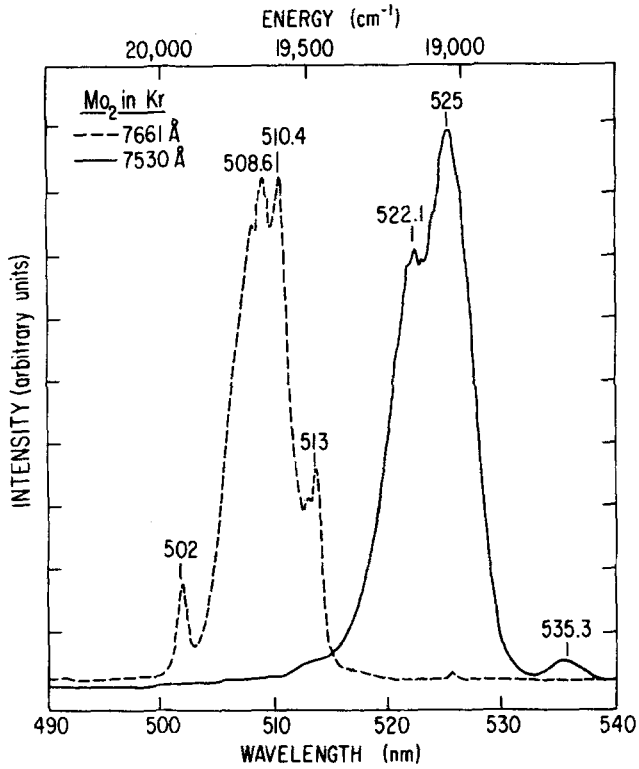

FIG. 13. Excitation spectra of Mo_2 in Kr. The solid curve is obtained by monitoring emission intensity at 753.5 nm and scanning the excitation frequency. The broken line is similarly derived except emission was monitored at 766.1 nm.

Additional analysis of the emission spectrum can be drawn from the excitation spectra (Fig. 13). Comparison with Fig. 10 shows that every absorption feature is represented in the excitation spectrum except for the 537.4 nm absorption feature. This aspect is similar to the absence of the 528.9 nm absorption peak from the Mo_2 excitation spectrum in Ar matrices.

Relative quantum yields for the two absorption sites can be found from the emission intensities since laser power varied only slightly (±5%) over this wavelength range. As with Ar matrices the blue site absorption has about a four times larger quantum yield than red site absorption. Absolute quantum yields are slightly larger than in Ar matrices but still on the order of 10^{-5}.

The time evolution of emission at 766.1 and 753.5 nm when excited at 510.6 and 527.4 nm, respectively, can be found in Fig. 14. Similar decays were elicited at a variety of excitation and emission wavelengths. Both decays show at least two exponential dependences. Again as in Ar the longer lifetime is associated with a lower quantum yield.

High resolution emission spectra show larger phonon interactions than their argon matrix counter parts (Figs. 15 and 16). Indeed, no distinct zero phonon line can be detected in emission at 724.5 or 753.5 nm. Emission at 739.1 nm shows only a barely resolved zero phonon line which is lost in the next emission peak at 766.1 nm. As in Ar matrices the lines substantially broaden as the progression moves toward lower emission energies.

TABLE II. Emission data of Mo_2 in Kr matrices at 13.5 °K.

Emission λ (Å)	Emission ν (cm⁻¹)	Excitation λ (Å)	Transition[c] ν′→ν″	FWHM (cm⁻¹)	$\Delta\nu=\nu_i''-\nu_{i+1}''$ (cm⁻¹)	
7274.3	13747.0	5274	0→0	...*		
7534.9	13271.6	5274	0→1	...*	475.4	
7812.1	12800.6	5274	0→2	...*	471.0	$\overline{\Delta\nu}$=476.5±4 cm⁻¹
8115.2	12322.6	5274	0→3	...*	478.0	
8445.1	11841.2	5274	0→4	...*	481.4	
7390.6	13530.7	5106	0→0	5.9		
7661.1	13052.9	5106	0→1	13.1	477.8	
7951.9	12575.6	5106	0→2	26.1[a]	477.3	$\overline{\Delta\nu}$ 475.3±3 cm⁻¹
8264.4	12100.1	5106	0→3	...[b]	475.5	
8599.2	11629.0	5106	0→4	...[b]	471.1	

[a]The zero phonon line is poorly resolved.
[b]The zero phonon line is not resolved.
[c]Tentative assignment.

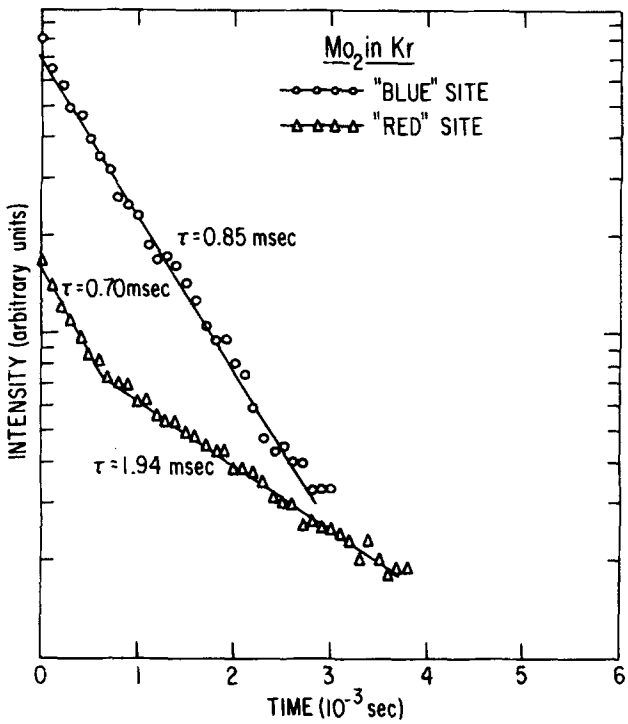

FIG. 14. Time evolution of emission at 766.1 nm produced by excitation at 510.6 nm (o). Also displayed is the time evolution of 753.5 nm emission produced by 527.4 nm excitation (Δ).

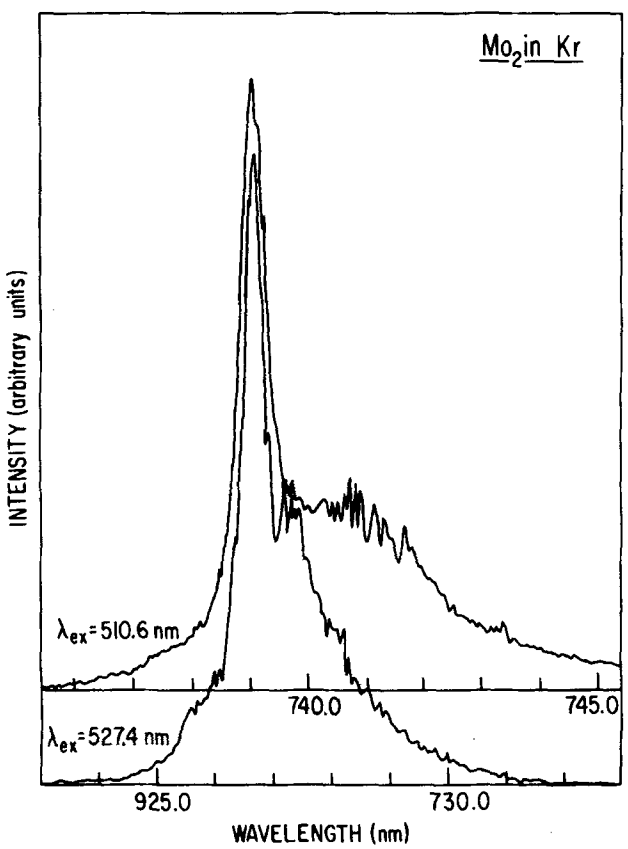

FIG. 15. Comparison of emission peak shapes from Mo_2 in a Kr matrix produced by excitation at 510.6 and 527.4 nm. The peaks are the highest energy emissions of their respective progressions.

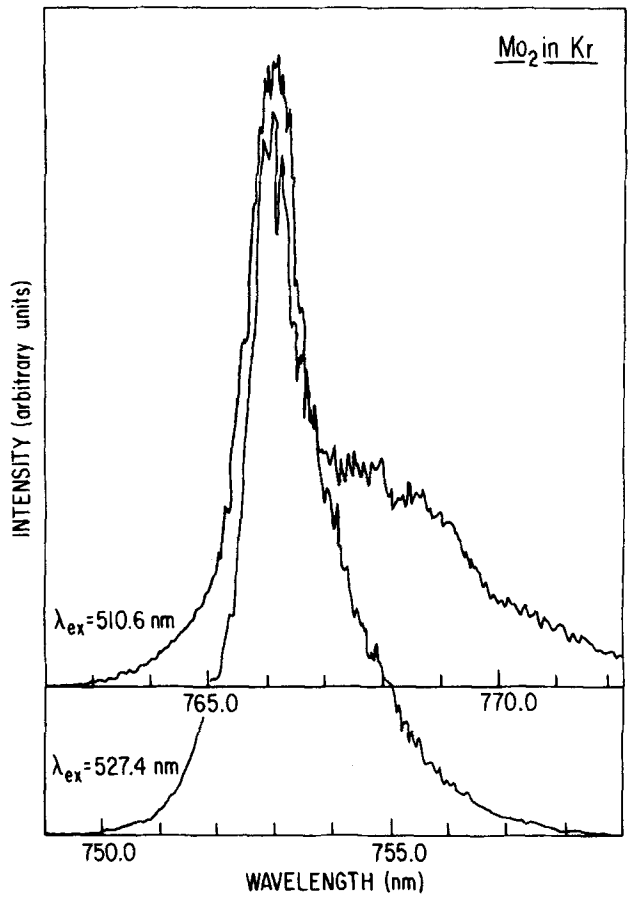

FIG. 16. Comparison of emission peak shapes from Mo_2 in an Ar matrix produced by excitation at 510.6 and 527.4 nm. The peaks are the second highest energy emissions of their respective progressions.

IV. ANALYSIS

The emission spectra of molybdenum doped argon and krypton matrices (Figs. 9 and 12) are indicative of the presence of two distinct matrix sites for Mo_2. A deconvolution of the absorption spectrum into individual components from the two sites is accomplished by means of the excitation spectra (Figs. 5 and 13). Since the annealing behavior of the two sites is different, spectra measured during annealing studies are also useful in giving information on site occupation (Fig. 11). The similarity of the emission spectra from the two sites in argon or krypton matrices shows that the electronic structures of Mo_2 in the two sites are only slightly affected by the matrix environment.

It is an over simplification to conclude that Mo_2 occurs in only two sites. Rather it is clear from the sharp zero phonon lines observed in fluorescence that the absorption bands are inhomogeneously broadened. Thus each "site" appears to be composed of a group of somewhat different Mo_2 molecular environments in the matrix. These arrangements are distinct enough to have the widely different fluorescent decay rates indicated by double and triple exponential time dependences for fluorescent emission (Figs. 6 and 14). Similar multiple site occupations have been observed for many atoms including Mo.[32] It would appear that further work on quantum

efficiency and fluorescent lifetime measurements could prove helpful in elucidating the details of host-matrix interactions particularly in regard to the characterization of the nature of different sites.

Although the overlapping absorption bands of Mo_2 in Ar and Kr matrices appear superficially to be quite different (Figs. 3 and 10), their shapes when deconvoluted into the individual site components (Figs. 5 and 13) are remarkably similar. The absorption bands for Mo_2 show peaks with small and irregular spacings. For instance, the blue absorption site of Mo_2 in an argon matrix has spacings of 53, 167, 75, 152, and 70 cm^{-1}. Since the emission spectrum is both regular and displays 475 cm^{-1} spacings, identification of the absorption peaks with excited state vibrational spacings implies a strongly perturbed excited state energy well. Although no other optically allowed excited state is present at this energy,[29] matrix interactions could couple the $^1\Sigma_u^+$ state with the dense manifold of higher multiplicity states located in this energy region producing the observed strong perturbation of vibrational structure.

An additional complication in the absorption spectrum is the presence (in most matrices) of another Mo multimer. Excitation spectra (Figs. 5 and 12) clearly show that the absorption peak appearing at 528.8 nm in argon and at 537.4 nm is krypton is not due to Mo_2 molecules. Annealing behavior as well as photoaggregation properties make an assignment of this species to Mo_3 attractive. Fluorescence from this species has not as yet been observed.

It is of interest to compare the peak assignments given here to those previously reported[21] for Mo containing argon matrices. In the present series of experiments structure is observed in the 500 nm region of the absorption spectra as had been previously reported.[17] This may well be due to slower deposition and thus more "crystalline" matrices in these experiments than in the work of Ozin and Klotzbücher.[16] It appears likely however that the 534 and 542 nm peaks previously assigned to Mo polymers[21] in argon matrix supports are in fact part of the Mo_2 absorption spectrum.

Some information about the nature of the two absorption sites can be derived from the emission data. In both Ar and Kr matrices the red absorption site is thermally more stable, and shows larger phonon interactions in its emission peaks compared to the blue site (Figs. 7, 8, 15, and 16). The time dependence of the emission can be used to test various models for the interaction of Mo_2 dimers with the surrounding matrix cage.

Clearly, the observed luminescence cannot emanate directly from the optically allowed $^1\Sigma_u^+$ state at 520 nm which is populated from the ground state by laser radiation. The lifetime of emission from either site in Ar or Kr matrices is far longer than expected for an optically allowed transition. Further, the shift in energy between excitation and emission photons is probably too large to be accounted for by a Stokes shift. Finally, consideration of the quantum yields and emission lifetimes of the red and blue absorption sites in Ar or Kr

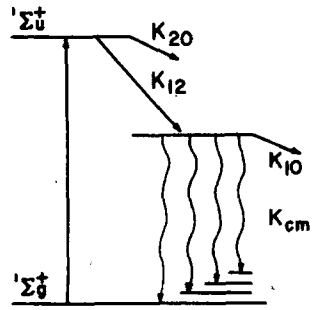

FIG. 17. Emission path for excited Mo_2. K_{12} may not be a single rate but rather a variety of couplings between 1 and 2. Kem is the emission rate to any of the ground state vibrational levels.

shows that the time dependence of emission is generally not a single exponential decay (see Figs. 6 and 14). However, the relationship $\tau_{blue} \leq \tau_{red}$ holds where τ is the lifetime of emission while blue and red refer to absorption sites. The measured quantum yield relationship between the two sites is $QY_{blue} \geq 4\,(QY_{red})$ where blue and red again refer to absorption sites. The quantum yield for direct emission from the $^1\Sigma_u^+$ excited state in either the red or blue site is related to the emission lifetime since $QY = \tau K_{rad}$ is the pure radiative decay rate. With $QY_{blue} \geq 4\,(QY_{red})$ the assumption of direct emission would lead one to conclude $K_{rad,blue} \geq 4\,(K_{rad,red})$. It seems highly unlikely that the small changes in electronic structure exhibited by Mo_2 in the two sites could be responsible for such a major change in oscillator strength.

A more plausible explanation for the origin of the observed emission can be found in Fig. 17. Excitation occurs along the optically allowed $^1\Sigma_u^+ \leftarrow {}^1\Sigma_g^+$ path. However, the $^1\Sigma_u^+$ state represents the highest energy state of a dense manifold of spin states having multiplicities as high as 13 and both π and Σ symmetries. The matrix environment can be expected strongly to couple these levels. Emission then would occur from a "trap" level which would have high spin multiplicity and be located at a lower energy than the initially excited $^1\Sigma_u^+$ state.

Emission from such a state could be both long-lived and strongly shifted to longer wavelengths with respect to the exciting wavelength. Furthermore, the emission path described in Fig. 17 does not require one to assume a major change in oscillator strength between Mo_2 in the red and blue sites as is the case for the direct emission model. Rather, in such a three level scheme the quantum yield and lifetime are related as $QY = K_{12}/(K_{12}+K_{10})\tau$, where K_{12} represents the rate at which Mo_2 decays from the optically excited $^1\Sigma_u^+$ state to the emitting trap level. K_{10} is the sum of all other decay rates of excited molecules from the optically excited level. Here τ represents the emission decay time and is $\tau = K_{rad}(K_{rad}+K_{20})^{-1}$ with K_{rad} being the pure radiative decay rate and K_{20} being the sum of all other decay processes from the emitting level (2). Thus the measured quantum yields ($QY_{blue} \geq 4\,QY_{red}$) and lifetimes ($\tau_{red} \geq \tau_{blue}$) requires only that one or a combination of the nonradiative rates (K_{10}, K_{12}, or K_{20}) are affected as a result of changing site distributions. The population of

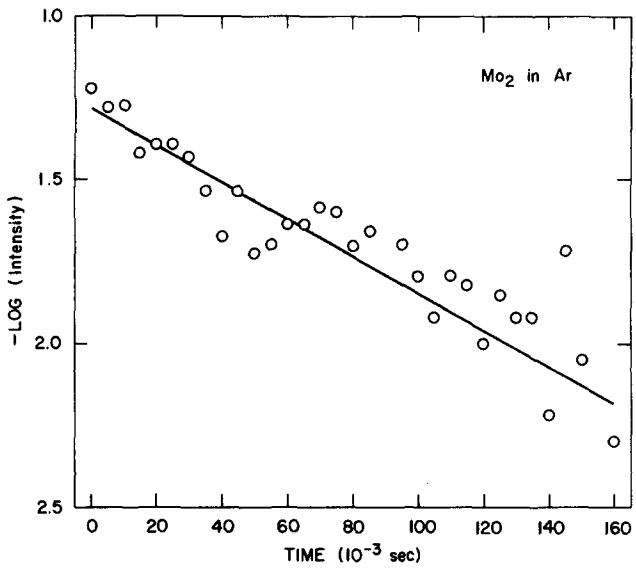

FIG. 18. Ground state repopulation as a function of time following excitation. The absorbance of Mo_2 in an Ar matrix was monitored at 517.8 nm following a 517.8 nm excitation pulse.

state 2 has complex kinetics which can be expressed as follows:

$$N_2(t) = N_1(0)K_{12}(K_{20} + K_{\text{rad}} - K_{10} - K_{12})^{-1} \times \{\exp[-(K_{10} + K_{12})t] - \exp[-(K_{\text{rad}} + K_{20})t]\} . \quad (1)$$

The population of state 2, the emitting state, is zero before excitation. The laser pulse which is short compared to the times of interest populates state 1 by exciting ground state atoms at time $t = 0$. The population in state 2 then increases at a rate $K_{10} + K_{12}$ [Eq. (1)]. Thus one might expect to observe an emission rise time. This rise time would be expected to be short since the rate K_{10} includes the direct radiative rate for the optically allowed $^1\Sigma_u^+ - {}^1\Sigma_g^+$ transition. The lack of detectable direct emission would further indicate that K_{12} is much larger than this pure radiative rate. Experiments designed to measure this rise time show it to be less than 1 μsec. The low light intensity made experiments with better time resolution inconclusive.

Emission appears to come from a single vibronic level since the spectrum due to a simple absorption site is unchanged over a broad range of excitation wavelengths. The emission lifetimes are much longer than typical vibrational relaxation times and the emission peak spacings are too large to represent differences in ground and excited state vibrational energies.

The lower electronic state in such an emission sequence need not be the ground state. As pointed out earlier Mo_2 has a variety of higher multiplicity states that lie in energy between the ground state and the $^1\Sigma_u^+$ state.[29,30] Evidence that the lower state in emission is indeed the ground state can be drawn from several sources. Figure 18 shows the time dependence of ground state repopulation following excitation. This experiment demonstrates that the return of the atoms to the ground state following excitation is on time scales commensurate with the emission lifetime. Unfortunately, the relatively poor signal to noise of this experiment does not allow any multiple exponential behavior to be distinguished. A second indication that the vibrational progression measured in these emission experiments is that of the Mo_2 ground state is in the agreement of the presently measured ω_e with that found in flash photolysis experiments.[23] In those experiments an emission progression with $\omega_e = 477.1$ cm^{-1} was tentatively identified as being due to ground state Mo_2. As well, the presently measured $\omega_e = 475.7\ (\pm 4.5)$ cm^{-1} is in good agreement with the best ground state *ab initio* calculations which predict $\omega_e = 475$ cm^{-1}.[14]

High resolution spectra of the zero phonon emission lines do not show resolved structure due to different isotopic species (Figs. 7, 8, 15, and 16). Natural molybdenum has six isotopes with greater than 9% natural abundance. Thus there are 21 Mo_2 isotopic species with appreciable abundance. It seems likely that the 7245 and the 7308 Å emission peaks observed in argon matrices as well as the 7274 and the 7390 Å emission peaks observed in krypton matrices correspond to the $v'' = 0$ vibrational level of the ground state since no emission could be detected on the high energy side of these peaks even with a three order of magnitude increase in detection sensitivity. Any other vibrational quantum number assignment would require strongly varying Franck–Condon factors for two adjacent vibrational levels. The existence of such strongly varying Franck–Condon factors is made more unlikely since the regular vibrational spacing observed in emission is indicative of a harmonic ground state energy well. It may be possible to get a feel for the relative ground and emitting state bond strengths from the widths of the emission lines in species having the lowest and highest vibrational frequencies ($Mo^{92}Mo^{92}$ and $Mo^{100}Mo^{100}$).

The energy difference exhibited by these two diatomics for vibronic transitions emanating from the lowest vibrational level of an excited electronic state $v' = 0$ and ending in an arbitrary vibronic level of the ground state v'' can be expressed in the harmonic oscillator approximation as

$$E_{\text{cm}^{-1}} = v''(K''^{1/2}[\mu_{92}^{-1/2} - \mu_{100}^{-1/2}]) + \tfrac{1}{2}(K'^{1/2} - K''^{1/2})(\mu_{92}^{-1/2} - \mu_{100}^{-1/2}) , \quad (2)$$

where K'' and K' are force constants for the ground and excited electronic state, respectively. μ_{92} and μ_{100} are the reduced masses of the two homonuclear diatomics. Thus a plot of the FWHM's of the zero phonon lines of the emission peaks versus v'' should be linear. An examination of Tables I and II shows that this is, indeed, the case. Under the assumption that the highest energy emission peak corresponds to $v'' = 0$ it is readily apparent from Eq. (1) that $\frac{1}{2}(K'^{1/2} - K''^{1/2})(\mu_{92}^{-1/2} - \mu_{100}^{1/2}) \leq 3$ cm^{-1} (the measured FWHM of 3.1 cm^{-1} is a convolution of the signal width with the spectrometer bandwidth). Thus $K' > K''$ but of the same order of magnitude as expected from theoretical predictions.[29] Any other ground state vibrational quantum number assignment (that is identification of the 7241 Å peak with $v'' > 0$) would indicate that the excited state force constant is smaller than the ground state's constant.

Tables I and II show that ω_e does not change within the experimental error of the measurements in going from the blue to the red site in either Ar or Kr matrices. A force constant of $1.62\times10^4\pm2\times10^2$ dyn cm^{-1} is indicated for $\omega_e=475.7\pm4.5$ cm^{-1}. By comparison the force constants for H_2, N_2, and Si_2 are 1.46×10^4 dyn cm^{-1}, 5.82×10^4 dyn cm^{-1}, and 5.41×10^3 dyn cm^{-1}, respectively.[34] The Mo_2 bond therefore represents one of the strongest diatomic bonds consistent with the measured $\Delta H^0_{298}=97\pm5$ kcal/mol.[28] A bond order as high as six is suggested from the results of extended Hückel molecular orbital and SCF–X–SW calculations.[7,12]

Mo_2 has by far the highest vibrational frequency among transition metal diatomics so far measured. Raman spectra of Zn_2,[35] Cd_2,[35] and Ag_2[36] indicate ω_e's of 80, 58, and 194 cm^{-1}. Absorption spectra indicate 110 and 194 cm^{-1} excited state vibrational spacings for Mn_2 and Fe_2.[32]

Certain empirical relationships between bond lengths and force constants have been noted for diatomic molecules.[34] While the constants derived are not directly applicable to transition metals, it is interesting to apply these rules to Mo_2. From $\omega_e=475.7\pm4.5$ cm^{-1} a bond length r_e of 1.90 ± 0.02 Å is indicated. From rotational information derived from flash photolysis experiments a bond length of 1.929 Å was deduced.[23] The force constant can be related to ΔH^0_{298} by another still another set of empirical rules,[37] which gives a computed value of $\Delta H=89$ kcal/mol comparing favorably with that determined from mass spectrometric measurements.[28]

[1]F. F. Abraham, *Homogeneus Nucleation Theory* (Academic, New York, 1974).
[2]J. F. Hamilton, J. Vac. Sci. Technol. **13**, 319 (1976).
[3]R. van Hardveld and F. Hartog, Adv. Catal. **22**, 75 (1972).
[4]See for instance, R. D. Adams and N. M. Golembeski, J. Am. Chem. Soc. **101**, 1307 (1979) and references therein.
[5](a) A. J. L. Hanlan and G. A. Ozin, Inorg. Chem. **16**, 2848 (1977); (b) A. J. L. Hanlan and G. A. Ozin, Inorg. Chem. **16**, 2857 (1977).
[6]M. Moskovits and J. E. Hulse, J. Phys. Chem. **81**, 2004 (1977).
[7]J. G. Norman, H. J. Kolari, H. B. Gray, and W. C. Trogler, Inorg. Chem. **16**, 987 (1977).
[8]M. D. Curtis, K. R. Han, and W. B. Butler, Inorg. Chem. **19**, 2096 (1980).
[9]J. V. Brencic and F. A. Cotton, Inorg. Chem. **8**, 7 (1969).
[10](a) D. Lawton and R. Mason, J. Amer. Chem. Soc. **87**, 921 (1965); (b) F. A. Cotton and J. G. Norman, J. Coord. Chem. **1**, 161 (1971).
[11]A. Bino, F. A. Cotton, and W. Kaim, Inorg. Chem. **18**, 3030 (1979).
[12]W. Koltzbücher and G. A. Ozin, Inorg. Chem. **16**, 984 (1977).
[13]W. Koltzbücher, G. A. Ozin, J. G. Norman, and H. J. Kolari, Inorg. Chem. **16**, 2871 (1977).
[14]B. E. Bursten, F. A. Cotton, M. B. Hall, J. Amer. Chem. Soc. **102**, 6348 (1980).
[15]P. M. Atha, I. H. Hillier, and M. F. Guest, Chem. Phys. Lett. **75**, 84 (1980).
[16]J. G. Norman, Jr. and P. B. Ryan, J. Comp. Chem. **1**, 59 (1980).
[17]C. Wood, M. Duran, I. H. Hillier, and M. F. Guest, Symp. Faraday Soc. (1980) (in press).
[18]D. W. Green and D. M. Gruen, J. Chem. Phys. **60**, 1794 (1974).
[19]W. D. Hewett, J. H. Newton, and W. Weltner, J. Phys. Chem. **79**, 2640 (1975).
[20]W. Koltzbücher and G. A. Ozin, Inorg. Chem. **16**, 984 (1977).
[21]G. A. Ozin and W. Klotzbücher, J. Mol. Cat. **3**, 195 (1977/78).
[22]J. K. Bates and D. M. Gruen, J. Mol. Spectrosc. **78**, 284 (1979).
[23]Y. M. Efremov, A. N. Samoilova, V. B. Kozhukhovsky, and L. V. Gurvich, J. Mol. Spectrosc. **73**, 430 (1978).
[24]K. Becker and M. Shurgers, Z. Naturforsch. A **26**, 2072 (1971).
[25]A. N. Samoilova, Y. M. Efremov, D. A. Zhuravlev, and L. V. Gusvich, Khim. Vgs. Energ. **8**, 229 (1974).
[26]Y. M. Efremov, A. N. Samoilova, and L. V. Gurvich, Opt. Spektrosck. **36**, 654 (1974).
[27]Y. M. Efremov, A. N. Samoilova, and L. V. Gurvich, Chem. Phys. Lett. **44**, 108 (1976).
[28]S. K. Gupta, R. M. Atkins, and K. A. Gingerrich, Inorg. Chem. **17**, 3211 (1978).
[29]W. A. Goddard, III (private communication).
[30]M. M. Goodgame and W. A. Goddard, III, California Institute of Technology, Arthur Amos Noyes Laboratory Contribution #6337, 1980.
[31]R. B. Wright, J. K. Bates, and D. M. Gruen, Inorg. Chem. **17**, 2275 (1978).
[32]C. Steinbruchel and D. M. Gruen, J. Chem. Phys. **74**, 205 (1981).
[33]D. Magde, J. H. Brannon, T. L. Cremers, and J. Olmsted, J. Phys. Chem. **83**, 696 (1979).
[34]R. F. Nalewski, J. Phys. Chem. **83**, 2677 (1979).
[35]A. Givan and A. Loewenschuss, Chem. Phys. Lett. **62**, 592 (1979).
[36]W. Schulze, H. N. Becker, R. Minkiwitz, and K. Manzel, Chem. Phys. Lett. **55**, 59 (1978).
[37]T. C. DeVore, A. Ewing, H. F. Franzen, and V. Calder, Chem. Phys. Lett. **35**, 78 (1975).